International Journal of Pharmaceutics 578 (2020) 119076

Contents lists available at ScienceDirect

International Journal of Pharmaceutics

journal homepage: www.elsevier.com/locate/ijpharm

Combination of Paclitaxel and R-flurbiprofen loaded PLGA nanoparticles suppresses glioblastoma growth on systemic administration

Secil Caban-Toktas[a], Adem Sahin[a,1], Sevda Lule[i,2], Gunes Esendagli[c], Imran Vural[a], Kader Karlı Oguz[d,e], Figen Soylemezoglu[f], Melike Mut[g], Turgay Dalkara[b], Mansoor Khan[h], Yilmaz Capan[a,*]

[a] Department of Pharmaceutical Technology, Faculty of Pharmacy, Hacettepe University, Ankara, Turkey
[b] Department of Neurology, Faculty of Medicine and Institute of Neurological Sciences and Psychiatry, Hacettepe University, Ankara, Turkey
[c] Department of Basic Oncology, Hacettepe University Cancer Institute, Ankara, Turkey
[d] Department of Radiology, Faculty of Medicine, Hacettepe University, Ankara, Turkey
[e] National Magnetic Resonance Research Center (UMRAM), Bilkent University, Ankara, Turkey
[f] Department of Pathology, Faculty of Medicine, Hacettepe University, Ankara, Turkey
[g] Department of Neurosurgery, Faculty of Medicine, Hacettepe University, Ankara, Turkey
[h] Texas A&M Health Science Center, Irma Lerma Rangel College of Pharmacy, Texas, USA
[i] Institute of Neurological Sciences and Psychiatry, Hacettepe University, Ankara, Turkey

ARTICLE INFO

Keywords:
Glioma
PLGA
Nanoparticles
Paclitaxel
R-flurbiprofen
Nanomedicine

ABSTRACT

Malignant gliomas are highly lethal. Delivering chemotherapeutic drugs to the brain in sufficient concentration is the major limitation in their treatment due to the blood-brain barrier (BBB). Drug delivery systems may overcome this limitation and can improve the transportation through the BBB. Paclitaxel is an antimicrotubule agent with effective anticancer activity but limited BBB permeability. R-Flurbiprofen is a nonsteroidal antienflammatory drug and has potential anticancer activity. Accordingly, we designed an approach combining R-flurbiprofen and paclitaxel and positively-charged chitosan-modified poly-lactide-co-glycolic acid (PLGA) nanoparticles (NPs) and to transport them to glioma tissue. NPs were characterized and, cytotoxicity and cellular uptake studies were carried out in vitro. The in vivo efficacy of the combination and formulations were evaluated using a rat RG2 glioma tumor model. Polyethylene glycol (PEG) modified and chitosan-coated PLGA NPs demonstrated efficient cytotoxic activity and were internalized by the tumor cells in RG2 cell culture. In vivo studies showed that the chitosan-coated and PEGylated NPs loaded with paclitaxel and R-flurbiprofen exhibited significantly higher therapeutic activity against glioma. In conclusion, PLGA NPs can efficiently carry their payloads to glioma tissue and the combined use of anticancer and anti-inflammatory drugs may exert additional anti-tumor activity.

1. Introduction

Brain tumors are highly lethal (Tzeng and Green, 2013). Among several subtypes of brain tumors, gliomas constitute the majority of primary malignant tumors in the central nervous system. They are highly aggressive and difficult to treat, hence, patients with glioma have a poor prognosis (Behin et al., 2003). Surgery is preferred if the tumor is operable and, is combined with radiotherapy and chemotherapy afterwards (Vredenburgh et al., 2009). However, operable gliomas are limited, because the boundaries of tumor tissue cannot easily be identified during surgery due to their infiltrative and invasive nature and, the risk of neurological dysfunction after resection could be

Abbreviations: API, Active pharmaceutical ingredient; BBB, Blood-Brain Barrier; CS, chitosan; FLUR, R-flurbiprofen; HPLC, high performance liquid chromatography; NP, Nanoparticle; NSAIDs, Non-steroidal anti-inflammatory drugs; PBS, Phosphate buffered saline; PEG, Poly-ethylene glycol; PLGA, poly-lactic-co-glycolic acid; PLGA-PEG, Poly-lactic-co-glycolic acid-polyethylene glycol copolymer; PTX, paclitaxel; PVA, polyvinyl alcohol; TPGS, alpha-tocopherol-PEG-1000 succinate

* Corresponding author at: Hacettepe University, Faculty of Pharmacy, Department of Pharmaceutical Technology, 06100 Ankara, Turkey.
E-mail addresses: gunese@hacettepe.edu.tr (G. Esendagli), imran@hacettepe.edu.tr (I. Vural), fsoyleme@hacettepe.edu.tr (F. Soylemezoglu), melikem@hacettepe.edu.tr (M. Mut), tdalkara@hacettepe.edu.tr (T. Dalkara), mkhan@tamu.edu (M. Khan), ycapan@hacettepe.edu.tr (Y. Capan).
[1] Present address: Department of Pharmaceutical Technology, Faculty of Pharmacy, Selcuk University, Konya, Turkey.
[2] Present address: Neuroscience Center and Department of Pediatrics, Massachusetts General Hospital and Harvard Medical School, Charlestown, MA 02129, USA.

https://doi.org/10.1016/j.ijpharm.2020.119076
Received 12 August 2019; Received in revised form 20 January 2020; Accepted 21 January 2020
Available online 24 January 2020
0378-5173/

substantial (Claes et al., 2007). Chemotherapy is instrumental in slowing down tumor progression and increasing the survival. Although several treatment strategies have been developed, more effective chemotherapy approaches are still needed in this field to improve the unfavorable prognosis.

Paclitaxel is an anticancer drug known to have an inhibitory effect against malignant gliomas in vitro (Fitzgerald et al., 2008). However, paclitaxel has low solubility, limiting its penetration to the brain. Designing a suitable pharmaceutical carrier can solve this limitation. Such a design should consider the technological parameters that can affect the size, loading capacity and the release of the chemotherapeutic drug in a controlled manner. The nanoparticles (NPs) prepared from the poly-lactic-co-glycolic acid (PLGA) polymer are highly suitable for this purpose because their technological characteristics and clinical reliability have been extensively investigated. On the other hand, chitosan (CS) is a linear polysaccharide with biodegradable and biocompatible properties. CS is preferred as a positively charged coating to facilitate the transport of payload by promoting interaction of NPs with negatively charged cell membrane. Cationic surface modification by CS can be achieved via electrostatic interactions with the negatively charged PLGA NPs. (Wang et al., 2013b).

Non-steroidal anti-inflammatory drugs (NSAIDs) are effective molecules frequently used in reducing pain and inflammation. Interestingly, aspirin and other NSAIDs have recently been found effective against colon cancer in in vitro and in vivo models (Rao et al., 1995; Reddy et al., 1996). R-flurbiprofen reduced tumor formation and progression in colon and prostate cancers in mice (Wechter et al., 1997; Wechter et al., 2000a). R-flurbiprofen also showed promising results in glioma cell cultures (King and Khalili, 2001; Wechter et al., 2000a; Wechter et al., 2000b). The anti-carcinogenic effects of R-flurbiprofen have been associated in part with regulation of signaling pathways converging on c-Jun N-terminal kinase (JNK) (Grosch et al., 2003), nuclear factor kappa B (NF-κB) (Tegeder et al., 2001) or p53 (Grosch et al., 2005). Moreover, R-flurbiprofen can suppress the reactive inflammation around gliomas, which may positively contribute to its antitumoral effect. However, like paclitaxel, R-flurbiprofen cannot effectively penetrate the brain when given systemically (Parepally et al., 2006).

Combination of paclitaxel with R-flurbiprofen and encapsulating them with NPs to overcome their physicochemical disadvantages may allow them to reach brain parenchyma in sufficient amounts to exert their potential anti-cancer activity. Since R-flurbiprofen and paclitaxel produce their anti-cancer activity through different pathways summarized above, their combination may offer an additive effect. Increasing evidence also suggests that inhibiting inflammation in cancer therapy plays a decisive role in tumor regression (Todoric et al., 2016). Additionally, p53 inactivation is reported to be correlated with a more invasive phenotype of glioblastoma (Djuzenova et al., 2015). Therefore, combining a potential activator of p53 like R-flurbiprofen may further promote the antigliomal activity of paclitaxel. To our knowledge this is the first preclinical study targeting the clinical use of this combination that may have additive antineoplastic effects. For this purpose, paclitaxel and R-flurbiprofen were separately loaded into NPs that were prepared with polymers of different characteristics. The characterization and cell culture studies were performed to select the most suitable formulation and in vivo efficacy assays were carried out in brain-tumorized rats.

2. Materials and methods

3-(4,5-Dimethylthiazol-2-yl)-2,5-Diphenyltetrazolium Bromide (MTT), Dimethyl sulfoxide (DMSO), Acetone, acetonitrile, Phosphate buffered saline (PBS) tablets, Poly-lactic-co-glycolic Acid (PLGA), polysorbate 80, R-flurbiprofen , propidium iodide and polyvinyl alcohol (PVA), alpha-tocopherol-PEG-1000 succinate (TPGS) were purchased from Sigma-Aldrich Co., USA. DMEM/Ham's F-12 liquid medium with stable glutamine, Penicillin/Streptomycin (liquid), (10x) Trypsin (1:250)/EDTA (0.5/0.2%) and fetal bovine serum (FBS) were received from BioChrom AG, Germany. DRAQ7™ was purchased from BioLegend, USA. Poly-lactic-co-glycolic acid-polyethylene glycol (PLGA-PEG) copolymer (RGP d 10105, Mw = 5000 g/mol, PEG 10%; 5000 Da) was puchased from Boehringer-Ingelheim, Germany. Ketamine (alfasan) and xylazine (alfamine) was purchased from Alfasan Int., Holland. Cyclosporin (Sandimmun) was purchased from Novartis, Switzerland. Highly pure chitosan salt (PROTASAN UP CL 113) was obtained from NovaMatrix, Norway.

2.1. Preparation of R-flurbiprofen and paclitaxel loaded and CS-coated NPs

NPs were formed according to nanoprecipitation method. TPGS and PVA concentration were determined through the preliminary studies. First, PVA (1%) or TPGS (0.02%) was dissolved in water. Then, the solution was filtered through 0.45 μm cellulose acetate membrane. Polymer (100 mg PLGA or PLGA-PEG) was dissolved in 5 ml acetone and added dropwise onto 10 ml of aqueous phase at 1100 rpm on magnetic stirrer to form NPs. Paclitaxel or R-flurbiprofen loaded NPs were prepared separately. Therefore, 5 mg of paclitaxel or R-flurbiprofen (active pharmaceutical ingredients: API) was dissolved in organic phase just before NP formation to prepare loaded PLGA NPs, whereas 3 mg of API was added into acetone to form PLGA-PEG NPs which was the maximum API concentration allowed formation of NPs without aggregation. CS was added into aqueous phase (TPGS or PVA solution) and dissolved to make a concentration of 1 mg/ml while preparing CS-coated NPs. After NPs were formed, the suspension was stirred overnight at 700 rpm on magnetic stirrer to evaporate the acetone. NPs were washed with 10 ml of water (twice for PVA emulsified NPs and once for the other formulations) and collected through centrifugation at 13500 rpm for 60 min. Supernatants were discarded after centrifugation and NPs were resuspended in 7 ml of water. NP were frozen at −20 °C overnight and freeze-dried at −80 °C with Heto Power Dry PL 3000 (Denmark) for 24 hr.

2.2. Characterization of NPs

2.2.1. Determination of particle size and surface charge of NPs

Particle size and polydispersity index values of NPs were determined from NP suspension diluted 1/20 with water, on the other hand the zeta potential values were determined from lyophilized NPs suspended in water by using Zetasizer Nano ZS (Malvern Instruments, UK). The measurement angle was set 173° and measurements were performed in triplicate. Scanning electron microscopy (SEM) was used to evaluate the morphological structure of NPs. Briefly, NP suspension prepared from lyophilized NPs was added onto carbon grid and let dry in room temperature. Samples were coated with gold (Quorum Technologies, SC7640 Auto/Manual High Resolution Sputter Coater, USA) and photographs were captured with SEM (FEI, NovaNanoSEM 430, USA).

2.2.2. Quantitative analysis of paclitaxel and R-flurbiprofen, evaluation of encapsulation efficiency and in vitro release studies

Quantification of paclitaxel and R-flurbiprofen was performed by high performance liquid chromatography (HPLC) (Agilent 1200 Series, USA) with a reversed-phase column (Inertsil® ODS-3, Particle size 5 μm, 4.6 × 250 mm, GL Sciences, China). Separate methods were carried out to determine the concentration of paclitaxel and R-flurbiprofen. The conditions were given in Table 1.

The encapsulation efficiency determined directly from lyophilized NPs. Briefly, NP powder was dissolved in DMSO to make a clear solution with a concentration of 1 mg/ml NP. Total encapsulated amount was acquired by comparing the concentration obtained from HPLC with NP batch yield. Encapsulation efficiency values were calculated according to the equation (Zhang and Feng, 2006):

Table 1
The chromatographic conditions of quantifying APIs.

Conditions	Paclitaxel	R-flurbiprofen
Mobile phase	Water:Acetonitrile (48:52)	Acetonitrile:0.1 M Acetate buffer (40:60)
Temperature	25 °C	25 °C
pH	–	6.8 (o-phosphoric acid)
Flow rate	1 ml/min	1 ml/min
Wavelength	227 nm	247 nm
Injection volume	20 µl	25 µl
Run time	20 min	12 min

% Encapsulation efficiency = (Actual amount of drug loaded in NPs/Total drug added) ∗ 100

In vitro release studies was performed with dialysis membrane method (Yang et al., 2007). Due to the difference of the solubilities of the APIs, release mediums were selected separately to provide the sink condition. The release medium for paclitaxel-loaded NPs was PBS containing 0.5% polysorbate 80 (15 ml/1 mg NP), whereas for R-flurbiprofen-loaded NPs was PBS (10 ml/1 mg NP) only. NP suspension in release medium was transferred into the dialysis bags and placed into sample tubes. Tubes were fixed into horizontal shaking water bath at 37 °C and samples were taken at predetermined time intervals.

2.2.3. Differential scanning calorimetry

Paclitaxel, R-flurbiprofen, physical mixture of polymer + API (drug/polymer ratio: 1/3) and API loaded particles were analyzed with DSC to investigate the possible interactions and incompatibilities between the polymer and active substances. Samples were transferred into aluminium pans and thermograms were obtained with DSC Q 2000 (TA Instruments with refrigerated cooling system T-90, USA). Paclitaxel samples were heated from 20 °C to 250 °C whereas temperature range changed for R-flurbiprofen samples to 20–140 °C at a heating constant rate 20 °C/min.

2.2.4. Fourier-Transform infrared spectroscopy (FTIR) analysis

FTIR analyses were performed to detect possible chemical interactions between the APIs and polymer during NP formation. The samples were prepared likewise with the DSC analysis. Paclitaxel, R-flurbiprofen, polymer (PLGA) and API loaded particles were analyzed with FTIR to investigate the possible interactions between the polymer and active substances. Samples were analyzed directly by inserting between the clips of the device (Bruker Alpha FTIR spectrophotometer, Germany). The spectra were recorded at 400–4000 cm-1 wavelength.

2.3. Cell culture studies

Cell culture studies were carried out to evaluate cytotoxicity and uptake characteristics of NPs. Rat glioma (RG2) cell line (ATCC, LGC Promochem, Rockville, MD, USA) was used for cytotoxicity studies. D-glucose (3151 mg/L), fetal bovine serum (FBS, 10%), L-glutamine (365.3 mg/L), penicillin–streptomycin (50 U/mL–50 µg/mL) containing (1:1) (DMEM/Ham's F-12; Dulbecco's Modified Eagle's Medium/Ham's Nutrient Mixture F-12) was used as cell culture medium.

For cell viability assays, RG2 cells (5×10^3/well) cells were seeded into 96-well flat-bottom plates and cultured for 24 h for initial attachment. Then, the cells were treated with the formulations and incubated for 48 h. NPs were added onto RG2 cells to make a concentration approximately 30 µM for both paclitaxel and R-flurbiprofen. Methyl thiazolyl tetrazolium (MTT, 5 mg/ml in PBS) was added into the wells, and incubated for 4 h. Then, the cells and formazan crystals were dissolved with a lysis buffer containing DMSO for 16 h. The optical density at 570 nm was recorded and the amount of viable cells was calculated as a percentage in comparison to that of the control cells cultured in culture medium alone.

Propidium iodide (PI)-loaded NPs were used to evaluate the cellular uptake. PI was preferred because it is a membrane impermeable dye and its signaling properties enhanced after interaction with DNA/RNA. Therefore, leakage from the NPs would not modify the results because the extracellular PI will not be fluorescent. PI loaded NPs were prepared with the same method, but the added amount into the NP formation medium was reduced because of aggregation. Therefore, 1 mg of PI was added to the organic phase before NP formation. For cellular uptake studies, RG2 cells (10^6/well) were seeded into 6-well plates and incubated for 24 h. Then, the culture media were removed and the NPs were added into the wells and the uptake was monitored at 3 h and 6 h. The cells were harvested and DRAQ-7 viability dye which emits a red fluorescence distinguishable from that of PI, was added to discriminate dead and viable cells. Analyses were performed on a flow cytometer (FACSAria II, Becton Dickinson, San Jose, CA, USA).

2.4. In vivo studies

2.4.1. Animals

The in vivo study protocol was approved by Hacettepe University Animal Experiments Local Ethics Committee (No. 2014/42-02). Sixty-six adult female Wistar rats (250–300 g) were housed in a standard animal facility under controlled temperature, humidity with a regular lighting schedule of 12 h light and 12 h dark, and fasted overnight, however were permitted free access to water before the experiment. All experiments were carried out in accordance with institutional guidelines.

Rats were anesthetized with intraperitoneal 40 mg/kg ketamine (100 mg/mL) and xylazin (16 mg/mL) mixture (with 2:1 ratio). Body temperature was continuously monitored by a rectal probe and maintained at 37.0 ± 1 °C with a thermal pat. Before the implantation of tumor cells, rats were administered with single dose/day cyclosporine in saline (1 mg/mL) for five days to depress the immune system, promoting the growth of tumor cells.

2.4.2. Implantation of RG2 cells

Tumor cell implantation was conducted according to the previous method (Sekerdag et al., 2017; Yemisci et al., 2006). Cells were incubated with 0.002% trypsin-0.005% EDTA solution for 2 min and fresh medium was added to stop the trypsin activity. Cell suspension was centrifuged at 2000 rpm for 2 min and supernatants were discarded. Then, cells were resuspended with 5 µl of medium without FBS for each rat. Rats were placed in stereotaxic instrument (Lab Standard Stereotaxic, Stoelting, IL, USA). One centimeter incision was performed onto scalp to visualize the injection area. Cell suspension was injected slowly with a Hamilton syringe unilaterally into the right striatum through a burr hole with coordinates from bregma; lateral 2 mm and posterior 4 mm with a 6 mm depth. After implementation, scalps were suturated and rats were followed up for daily activities. The schematic illustration of the procedure was shown in Fig. 1.

2.4.3. Magnetic resonance imaging (MRI)

To determine the presence and size of tumor, magnetic resonance imaging was performed with 3 Tesla MR unit (Magnetom Trio, Siemens Healthcare, Erlangen, Germany; slew rate, 200 mT/m/ms; maximum amplitude, 45 mT/m) in National Magnetic Resonance Research Center (UMRAM). Rats were investigated with MRI 10 days after the implantation of tumor cells to check if the solid tumor tissue present. Only the animals developing brain tumors at 10th day were included in the study. For this purpose, a handmade coil was developed by UMRAM and placed on a semi-cylinder body to support the rat body. The area of tumor was calculated by multiplication of the width and length obtained from MRI images. Then, rats were divided into the following experimental groups. All groups were administered with a single dose treatment containing 300 µg/kg for paclitaxel and 1.5 mg/kg for R-flurbiprofen via i.p. route. Five days after administration, MRI studies repeated to investigate the difference of the tumor area. T2-weighted

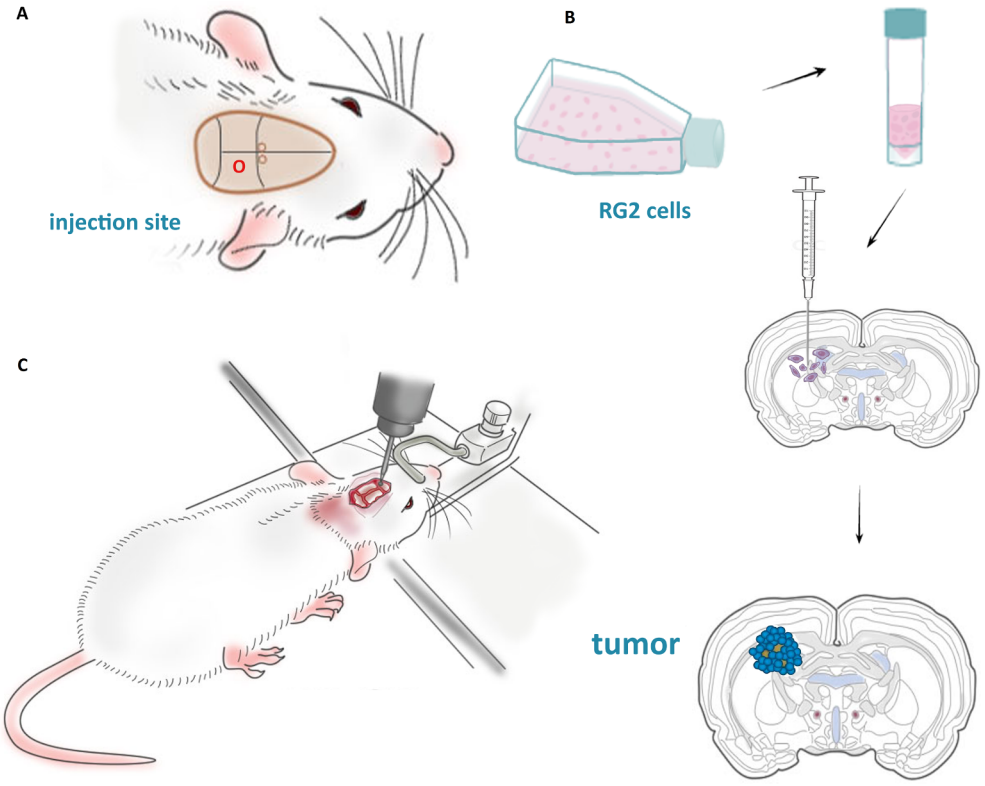

Fig. 1. Implantation of tumor cells. A, Incision was performed onto scalp to visualize the injection area. B, Fresh RG2 cell suspension was centrifuged in medium without FBS. C, Rats were placed in a stereotaxic instrument and the syringe was adjusted for the target coordinates. RG2 cell suspension was injected slowly with a Hamilton syringe unilaterally into the right striatum. Implantation was confirmed with MRI 10 days after the operation.

turbo spin-echo imaging was obtained parallel to the long-axis of the rat in prone position (coronal plane) using the following parameters: repetition time/echo time: 4420/94; field of view: 78 × 78 mm; slice thickness: 2 mm; interslice gap: 0; number of excitations: 5.

Illustrative abbreviations of experimental groups were;

- Control (Sham, n = 7)
- Paclitaxel solution (n = 8) (PTX Sol.)
- Paclitaxel and R-flurbiprofen solution (n = 7) (PTX&FLUR Sol.)
- TPGS emulsified NPs (blank) (n = 7) (Blank NPs (TPGS))
- PVA emulsified NPs (blank) (n = 8) (Blank NPs (PVA))
- TPGS emulsified NPs (paclitaxel-loaded) (n = 8) (PTX loaded NPs (TPGS))
- PVA emulsified NPs (paclitaxel-loaded) (n = 6) (PTX loaded NPs (PVA))
- TPGS emulsified NPs (paclitaxel & R-flurbiprofen-loaded) (n = 8) (PTX&FLUR loaded NPs (TPGS))
- PVA emulsified NPs (paclitaxel & R-flurbiprofen-loaded) (n = 7) (PTX&FLUR loaded NPs (PVA))

2.5. Histopathological analysis

After the second MRI experiment, rats were sacrified to perform histopathological analysis. The brains of rats were removed carefully and fixed in 10% formalin. Coronally sectioned 2 mm thick brain slides were embedded in paraffin. Serial 6 μm thick sections were stained with hematoxylin and eosin. The diameters of tumors (largest transverse and longitudinal) were determined at 4x magnification with a light microscope (LEICA, DM 3000 LED, Wetzlar, Germany).

2.6. Statistical methods

Statistical analysis were performed to compare the experimental groups. Kolmogorov-Smirnov normality tests were performed to identify the groups in which the data showed non-normal distribution and select the suitable test for the comparison. Normal distribution groups were compared with paired samples *t*-test, on the other hand, the remaining groups were compared with Wilcoxon test for paired samples with SPSS (IBM SPSS Statistics Ver. 20). Values of $p < 0.05$ were considered statistically significant.

3. Results

3.1. Particle size, morphology and zeta potential values of NPs

NPs were formed according to nanoprecipitation method and all particle size values were between 150 and 190 nm. The particle size values were given in Table 2. The polymer molecular weight and NP loading with paclitaxel or R-flurbiprofen did not cause any significant effect on the particle size. On the other hand, the particle size of the NPs emulsified with TPGS was smaller than NPs emulsified with PVA ($p < 0.05$). PEGylated NPs were significantly smaller than unmodified NPs and CS coating induced approximately 70 nm increase on the particle size ($p < 0.05$). All polydispersity index values were similar and lower than 0.2.

The SEM micrographs were given in Fig. 2 to show the morphology of NPs. All NPs were spherical and particle size values of NPs were consistent with the DLS measurements.

The zeta potential of NPs were shown in Table 3. All PLGA and PEGylated PLGA NPs possessed negative surface potential. NPs emulsified with TPGS had significantly denser negative potential than PVA emulsified NPs ($p < 0.05$). On the other hand, PEGylation or molecular weight of the polymer did not affect the zeta potential. The major alteration of the surface charge occurred when the NPs were coated with CS, which changed the surface charge of NPs from negative to positive.

3.2. Encapsulation efficiency of NPs

The encapsulation efficiency was investigated to determine the NP dosage given to the animals. Only the encapsulation efficiency values of the PEGylated NPs were determined because PEGylated NPs were used

Table 2
Particle size values of NPs prepared according to nanoprecipitation method.

	Polymer				
Formulation	PLGA (502H) NPs	PLGA (503H) NPs	PLGA (504H) NPs	PPG* NPs	CSP* NPs
Blank NPs (PVA)	187 ± 47	167 ± 2	177 ± 4	102 ± 3	172 ± 12
Blank NPs (TPGS)	145 ± 6	151 ± 2	157 ± 2	86 ± 3	158 ± 16
PTX loaded NPs (PVA)	185 ± 15	172 ± 6	184 ± 6	127 ± 15	188 ± 19
PTX loaded NPs (TPGS)	147 ± 2	155 ± 3	163 ± 7	118 ± 16	188 ± 29
FLUR loaded NPs (PVA)	173 ± 13	171 ± 7	174 ± 4	110 ± 4	186 ± 13
FLUR loaded NPs (TPGS)	144 ± 3	147 ± 5	150 ± 3	92 ± 4	166 ± 13

*PPG indicated NPs prepared with PLGA-PEG, on the other hand CSP was the NPs was prepared with PLGA-PEG and coated with CS. The values were given in nanometer (nm) and as mean ± standard deviation.

in vivo studies. As seen in Table 4, the amount of paclitaxel encapsulated into the NPs were higher than R-flurbiprofen. On the other hand, emulsification with TPGS resulted in slight increase in encapsulation. The yield after lyophilization for PLGA NPs varied between 80 and 95 %, on the other hand, the yield values decreased to 55–80% for PLGA-PEG NPs.

3.3. In vitro release studies

The release profiles of R-flurbiprofen or paclitaxel loaded PLGA-PEG NPs were shown in Fig. 3. Paclitaxel release from PLGA-PEG NPs continued to 5 days and reached a plateau. Approximately 60% of the paclitaxel was released from NPs. On the other hand, R-flurbiprofen was released relatively quickly and the release was finished at 6th hour. Release of APIs from CS-coated PLGA-PEG NPs demonstrated similar profiles with un-coated NPs. Surface coating with CS prolonged R-flurbiprofen release for 2 h more.

3.4. Differential scanning calorimetry (DSC)

DSC analysis was performed to determine possible chemical interactions after preparing the nanoparticular carrier system between the APIs and NP matrix. DSC analysis of the APIs and formulations were performed separately. According to the DSC thermograms, R-flurbiprofen possess an endothermic melting peak at 110 °C. This peak, also seen in the physical mixture, was not observed in R-flurbiprofen-loaded NPs (Fig. 4). Similarly, the DSC thermogram of paclitaxel demonstrated a melting peak at 220 °C. The subsequent peaks indicated that the sample was degraded immediately after melting.

3.5. Fourier-Transform infrared spectroscopy (FTIR) analysis

As seen in the spectrum of R-flurbiprofen (Fig. 5A), the wide peak observed between 2500 and 3300 cm^{-1} attributed to hydrogen bonds, peak from 1690 cm to 1 for carbonyl group and peaks near 1400 cm^{-1} for C—F streching. Similarly for paclitaxel (Fig. 5B), peaks around 3400–3250 cm^{-1} attributed to N—H strech, peak at 1750 cm^{-1} for C═O, peaks around 1250 cm^{-1} C—N strech and peaks at 690 cm^{-1} for aromatic ring. PLGA exhibited the peak indicating C—H stretching (3000–2850 cm^{-1}), and strong peaks from C═O (1750 cm^{-1}) and C—O stretching (1500–1000 cm^{-1}) related to the presence of the poly(lactic-co-glycolic acid) chains. Spectral analysis for API loaded NPs indicates that the functional groups of NPs and the chemical charactheristics were similar with API and polymer indicating that there was no chemical reaction between APIs and polymer matrix.

3.6. Cytotoxicity and uptake of NPs

In vitro cytotoxicity of API-loaded PLGA-PEG or CS-coated PLGA-PEG NPs were investigated on the RG2 cell line (Fig. 6). Blank NPs, TPGS or PVA coating did not show any significant difference, which indicated the absence of cytotoxic effects of NPs or CS coating on the cells. Expectedly, paclitaxel-loaded NPs displayed substantial cytotoxic effect when compared with the blank NPs (comparison was made separately for PLGA-PEG NPs and CS-coated PLGA-PEG NPs). R-flurbiprofen-loaded NPs exhibited cytotoxicity but the difference was not significant for all formulations.

Uptake of NPs were evaluated with PI-loaded NPs. In healthy cells, PI solution alone cannot breach the cell membrane therefore the only way for a cell to become fluorescent with PI is to allow the uptake of the NPs through the membrane. Simultaneously, DRAQ7 dye was also used to monitor the membrane integrity of the cells. PI-loaded NPs did not affect the viability of cells (Fig. 7A). The uptake occurred rapidly therefore difference between 3 h and 6 h was not substantial. TPGS coating enabled higher uptake compared with the PVA emulsified particles for both CS-coated and uncoated formulations ($p < 0.05$, Fig. 7B).

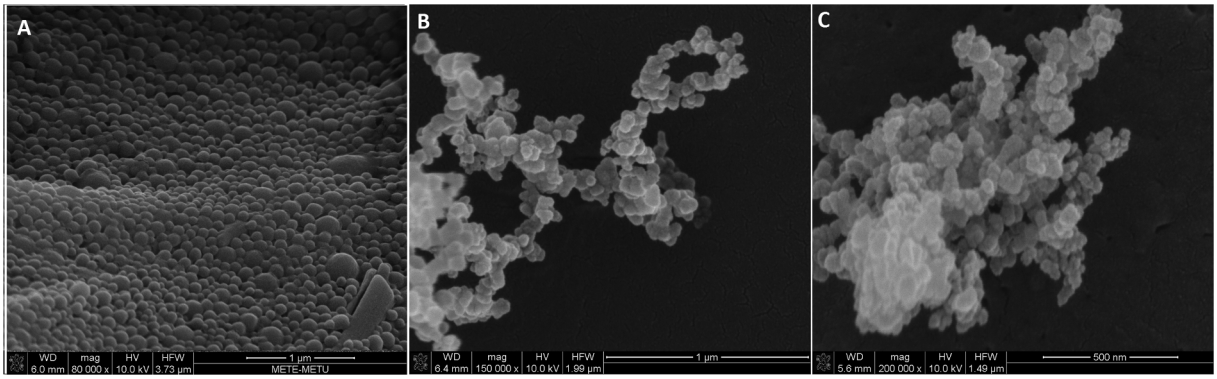

Fig. 2. The SEM micrographs of NPs. A, API loaded PLGA NPs. B, API loaded PEGylated PLGA NPs. C, API loaded CS-coated, PEGylated PLGA NPs.

Table 3
Zeta Potential Values of NPs.

	Polymer				
Formulation	PLGA (502H) NPs	PLGA (503H) NPs	PLGA (504H) NPs	PPG* NPs	CSP* NPs
Blank NPs (PVA)	−6.4 ± 2.5	−12.3 ± 4.6	−9.4 ± 5.6	−14.6 ± 1.1	32.7 ± 4.3
Blank NPs (TPGS)	−19.8 ± 3.5	−19.7 ± 4.6	−22.5 ± 3.7	−17.3 ± 1.8	31.4 ± 13.5
PTX loaded NPs (PVA)	−5.4 ± 2.2	−10.1 ± 5.4	−10.8 ± 3.7	−11.3 ± 2.5	36.5 ± 6.8
PTX loaded NPs (TPGS)	−20.5 ± 2.1	−16.4 ± 1.6	−17.3 ± 4.5	−18.2 ± 2.7	34.1 ± 21.7
FLUR loaded NPs (PVA)	−5.7 ± 1.3	−10.7 ± 5.6	−10.5 ± 5.5	−15.3 ± 1.3	47.8 ± 12.5
FLUR loaded NPs (TPGS)	−23.3 ± 3.1	−21.1 ± 6.1	−20.8 ± 1.8	−15.0 ± 0.9	38.2 ± 19.9

*PPG indicated NPs prepared with PLGA-PEG, on the other hand CSP was the NPs was prepared with PLGA-PEG and coated with CS. The values were given in millivolt (mV) as mean ± standard deviation.

Table 4
Encapsulation efficiency values of PLGA-PEG and CS-coated PLGA-PEG NPs.

Formulation	PPG* NPs (%)	CSP* NPs (%)
PTX loaded NPs (PVA)	49.1 ± 14.1	62.8 ± 11.3
PTX loaded NPs (TPGS)	61.9 ± 19.5	78.5 ± 10.8
FLUR loaded NPs (PVA)	35.7 ± 8.2	39.5 ± 8.6
FLUR loaded NPs (TPGS)	46.8 ± 4.8	44.9 ± 5.3

*PPG indicated NPs prepared with PLGA-PEG, on the other hand CSP was the NPs was prepared with PLGA-PEG and coated with CS. The values were given as mean ± standard deviation.

3.7. In vivo experiments

The difference between the tumor occupied areas of the rats were investigated with MRI to evaluate the efficacy of the formulations and the combination of paclitaxel and flurbiprofen. The pre-treatment and post-treatment MRI images of the samples from the experimental groups are given in Fig. 8. The control group (sham) and animals administered with paclitaxel solution, R-flurbiprofen solution and blank NPs showed dramatic increase of the tumor area over 5 days as seen in Fig. 9. On the other hand CS-coated PLGA NPs allowed the APIs to reach to the tumor and reduce the tumor area. According to the plain area values illustrated in Fig. 10; paclitaxel-loaded NPs reduced of the tumor size but the difference was not significant compared with the control group. Combination of paclitaxel-loaded NPs with R-flurbiprofen-loaded NPs resulted significantly higher reduction of the area and also total recovery in some animals (the final area of the tumor was 0 for four out of eight animals for the combined and TPGS emulsified NPs administered group, and two out of seven animals for combined and PVA emulsified NPs administered group). Additionally, R-flurbiprofen and paclitaxel loaded NPs, which were prepared with TPGS induced a significant decrease of the tumor area after post-administration compared with the control group. The pre-treatment tumor area values were statistically not different when all treatment and control groups compared (All p values were higher than 0.05). The post-treatment area values of the combination groups were compared with the post-implantation MRI of the control group and the difference was significant (p values were 0.028 and 0.037 for the combined NPs emulsified with TPGS and combined NPs emulsified with PVA respectively).

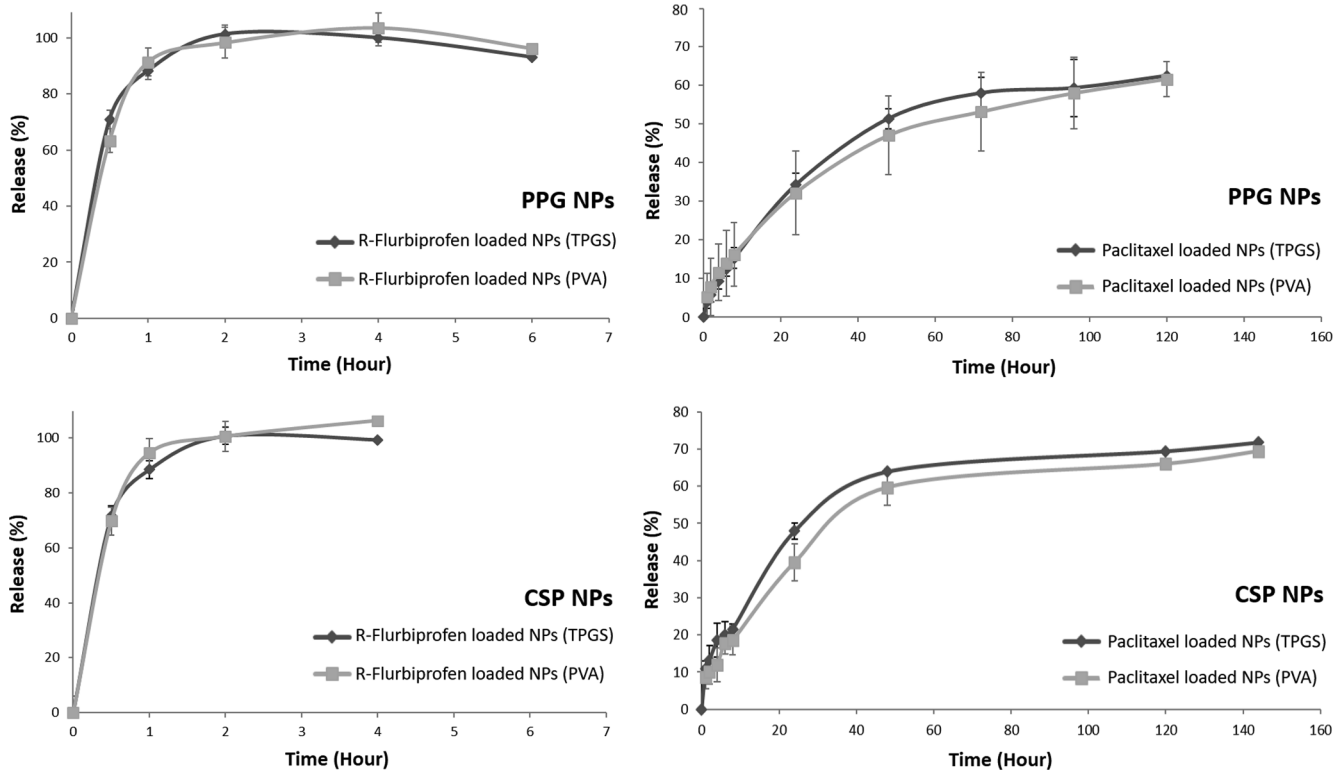

Fig. 3. Release profiles of APIs from NPs. R-Flurbiprofen was released with an initial burst and the release reached a plateau at 100% of the content near the 4th hour. On the other hand, paclitaxel release slowly continued through 5 days and the released content reached to 60–70%.

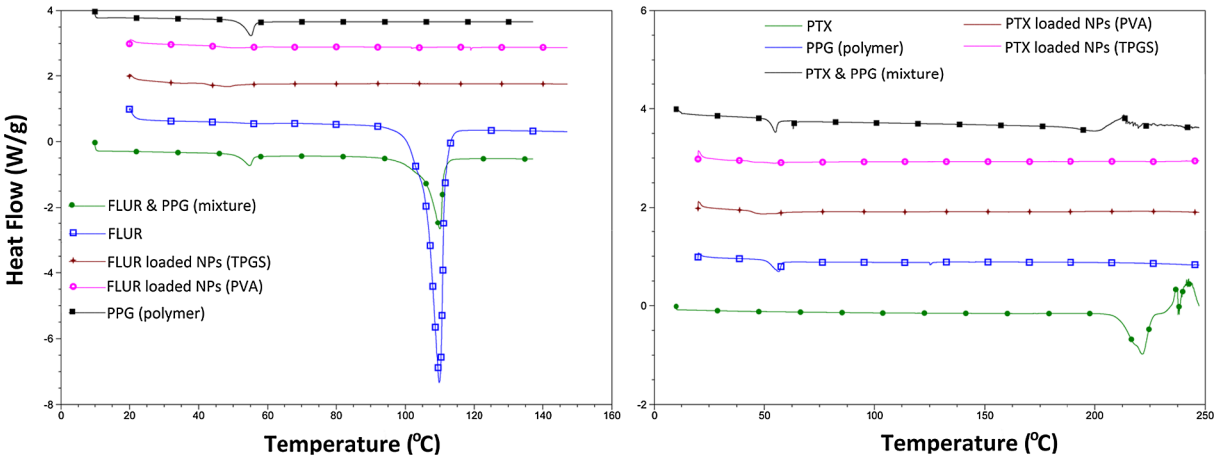

Fig. 4. The DSC thermograms of APIs and API loaded NPs. R-flurbiprofen alone and the physical mixture displayed an endothermic melting peak at 110 °C, whereas paclitaxel demonstrated a melting peak at 220 °C. The thermograms of API loaded NPs did not exhibit any other peaks, which indicated that the cargo (APIs) was loaded into the NPs through physical interactions without chemical bondings.

3.8. Histopathological analysis

Following the second MRI which was performed 5 days after treatment, the isolated brains were prepared for Hematoxylin-Eosin staining. Increased necrosis, hemorrhage, inflammation, reactive histiocytes and reactive glial cells were detected in the tumoral and peritumoral area (Fig. 11e and f). However, in the brains obtained from the combination group and the group that received only the paclitaxel NPs, the inflammatory response was further reduced. In combination groups, the tumor size as well as the associated pathological changes were all regressed (Fig. 11a and b). However, both paclitaxel-loaded NPs and paclitaxel and R-flurbiprofen solution administered animals demonstrated reactive cells along with the associated necrosis and hemorrhage.

4. Discussion

Glioma is an aggressive form of brain tumor and comprises of approximately 80% of primary malignancies in the central nervous system. Limitations in the treatment of these tumors and poor prognosis adversely affect the quality of life of glioma patients. The conventional method of glioma treatment involves chemotherapy and radiotherapy following surgery but there is a high risk of relapse after surgical operations. Although the probability of survival in high-grade glioma patients is improved by chemotherapy, the success rate is insufficient even in the best-responding cases. Therefore, new drug delivery strategies are needed.

The main purpose of this study was to design an effective biodegradable polymeric carrier system, which can be prepared by a relatively simple method and has high loading capacity for treatment of glioma. To ensure antiglioma activity, paclitaxel, which is used extensively in the treatment of several cancers, was selected as the main active drug and combined with anti-inflammatory R-flurbiprofen to enhance its antitumoral activity.

NP formulations were prepared by nanoprecipitation. For this, the biodegradable polymer and hydrophobic drug molecule were dissolved in an organic solvent, which is miscible with water, and this phase was added to the aqueous phase. By diffusion of the organic solvent into the aqueous solution, solid particles were formed and the organic solvent was subsequently evaporated. Polymeric drops quickly solidify and form particles due to the low solubility of the polymer in water (Wang et al., 2013a). Preparing NPs with nanoprecipitation was relatively simple because the formation occurred in one step (high speed homogenization was not needed). The particle size could be adjusted by changing the miscibility of organic solvent, concentration of polymer and ratio of the organic and aqueous phases (Cheng et al., 2007). The polymer concentration was selected as 20 mg/mL and, the organic phase: aqueous phase volume ratio was 1: 2 in order to keep the particle size within the intended range and to ensure adequate encapsulation.

Surfactants such as PVA and TPGS were used as emulsifiers and stabilizers while preparing PLGA NPs (Feng and Huang, 2001; Wang et al., 2013a). In particular, PVA is a surfactant used in different studies to provide a relatively small and uniform particle size (Mu and Feng, 2003b). TPGS is preferred for its high hydrophilicity, emulsifying

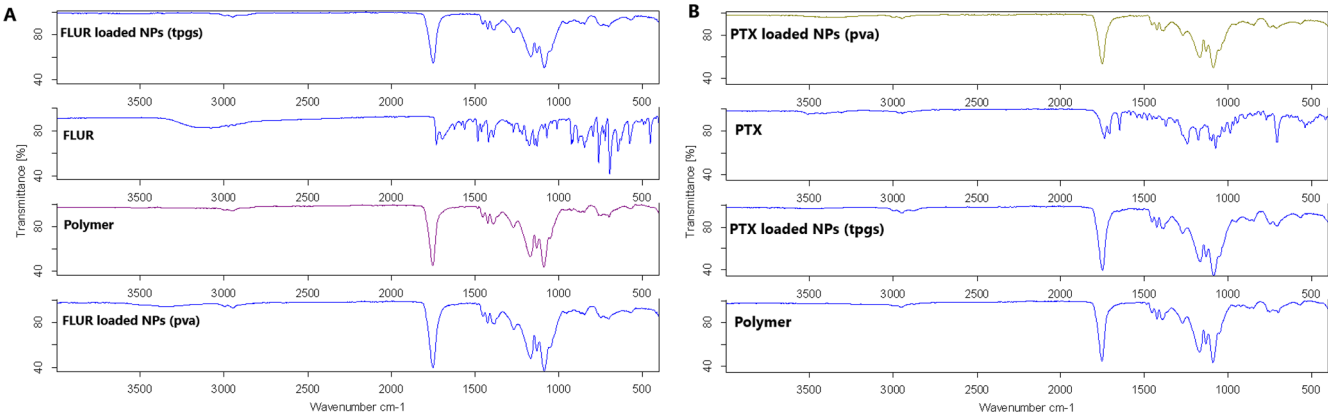

Fig. 5. The FTIR spectra of paclitaxel and R-flurbiprofen, API loaded PLGA NPs and polymer (PLGA).

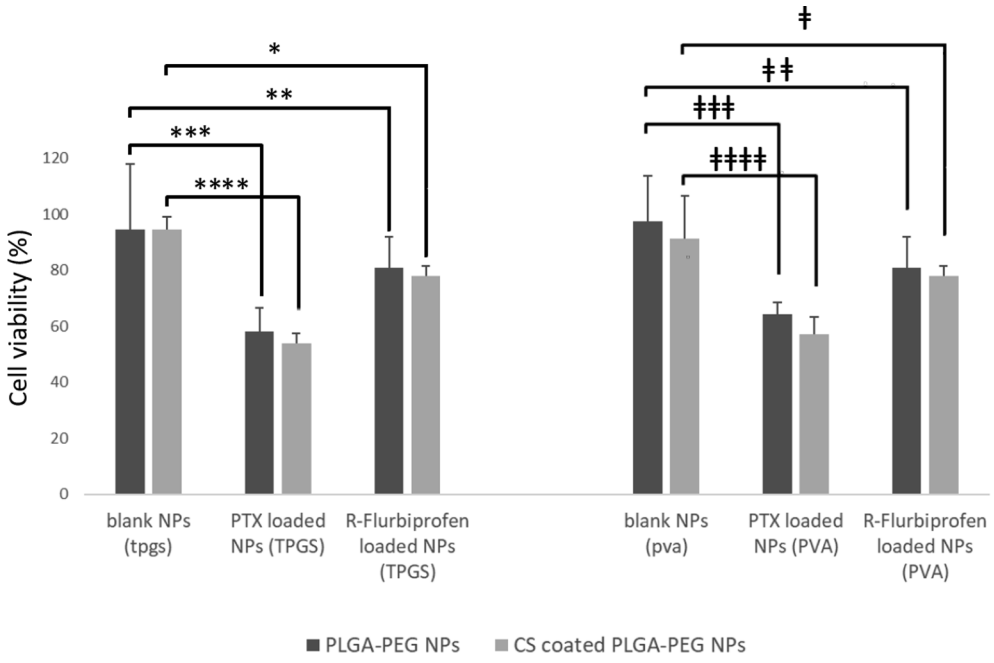

Fig. 6. In vitro cytotoxicity studies of NPs on RG2 cell line. Blank NPs did not cause any cytotoxic effect, whereas all paclitaxel-loaded NPs showed cytotoxicity (p values for *: 0.004, **: 0.341, ***: 0.063, ****: 0.0002 and ǂ: 0.210, ǂǂ: 0.217, ǂǂǂ: 0.026, ǂǂǂǂ: 0.022).

activity and membrane penetration enhancing capability (Mu and Feng, 2002, 2003a,b). Accordingly, anti-neoplastic carrier systems prepared with TPGS increased the in vivo therapeutic activity (Shieh et al., 2011). In our study, PVA was used at a concentration of 1% while preparing NPs. In the literature, different concentrations of PVA were used during PLGA NP preparation (Cruz et al., 2010; Feng and Huang,

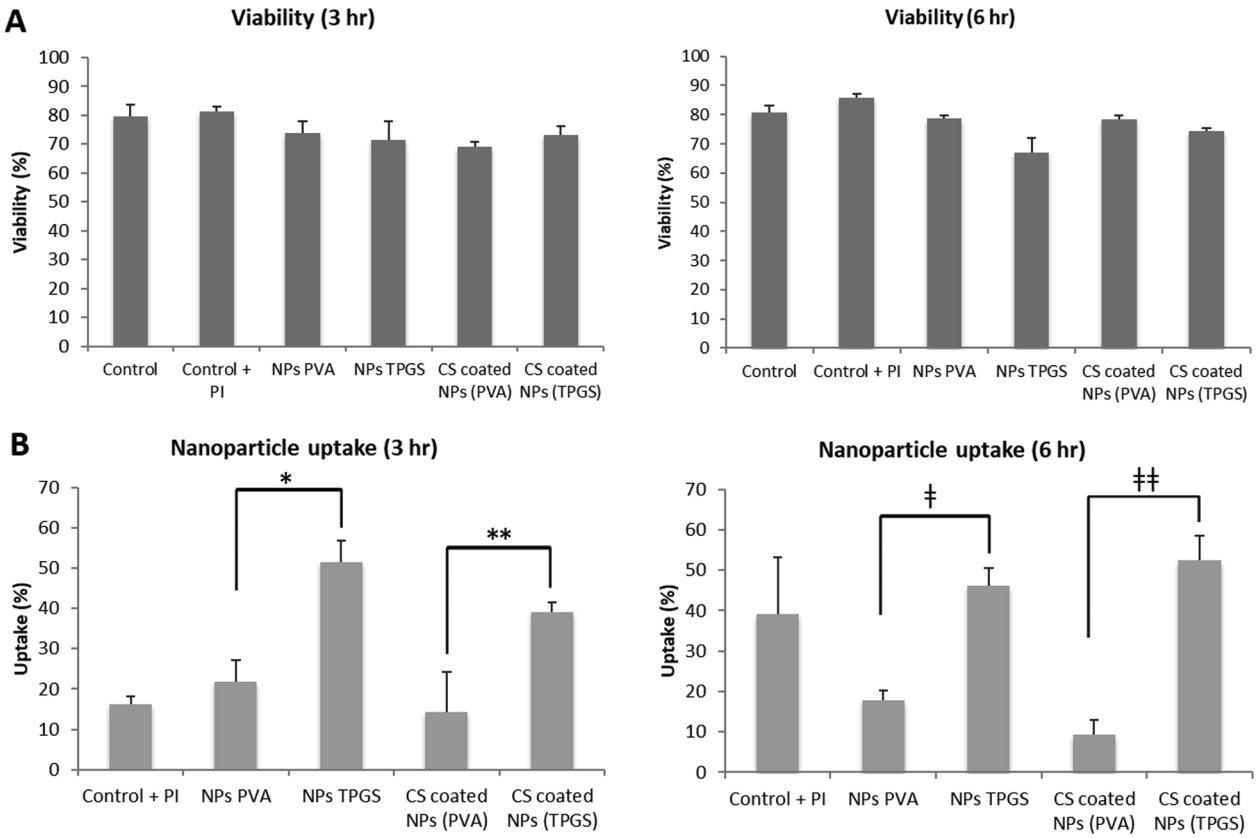

Fig. 7. The viability of RG2 cells and uptake of CS-coated and uncoated NPs. A, The graph shows that the propidium iodide (PI)-loaded NPs and free PI solution did not possess any significant effect on the viability of RG2 cells. B, Uptake of NPs occurred quickly thus there was no significant difference of internalizing of NPs into cells between 3rd and 6th hours. Additionally, NPs emulsified with TPGS were rapidly internalized and exhibited higher uptake (p values for *: 0.001, **: 0.006 and ǂ: 0.0003, ǂǂ: 0.0002).

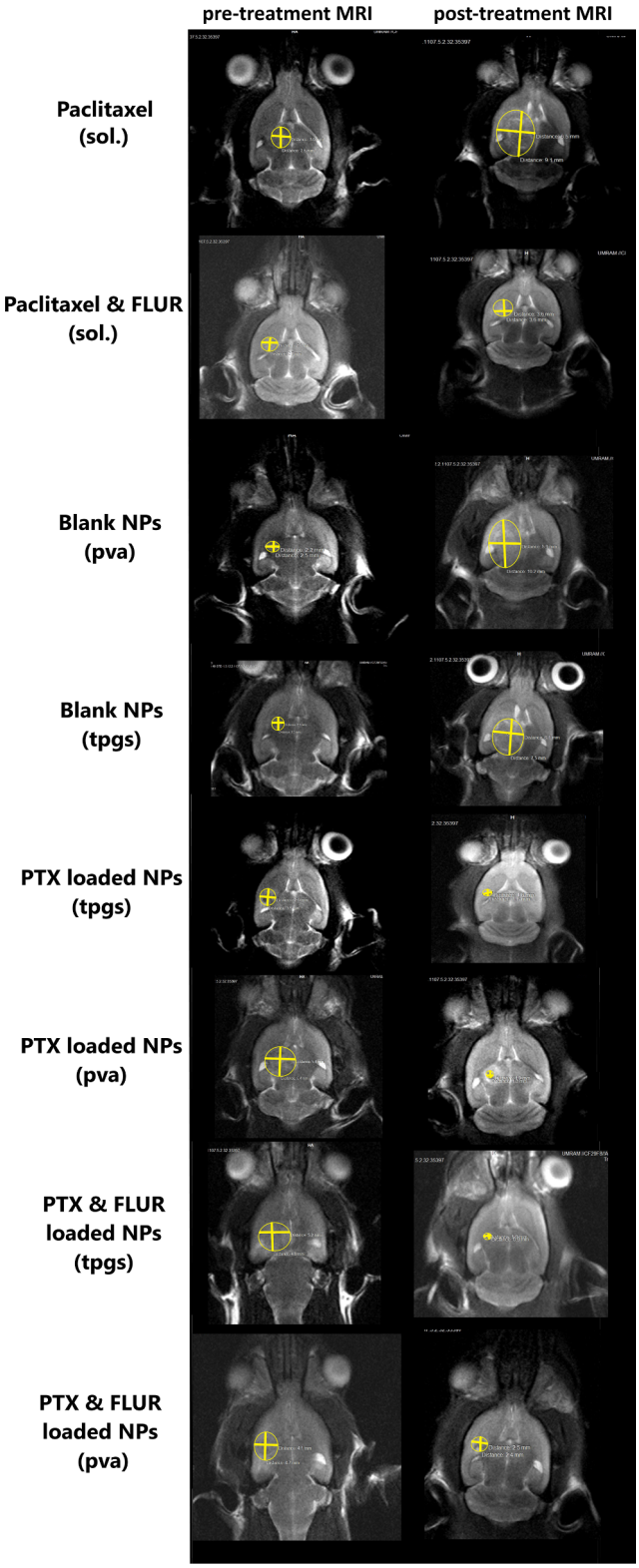

Fig. 8. The MR images from the experimental groups. The tumor size of treatment groups, which were administered with the API-loaded particles were decreased, whereas animals from the control groups (rats receiving blank NPs or API solutions) all exhibited tumor expansion. Figures were cut down to similar sizes for illustrative purposes, the image was rearranged and the boundaries of the glioma was emphasized with yellow marks. (For interpretation of the references to colour in this figure legend, the reader is referred to the web version of this article.)

2001; Kirby et al., 2013; Pamujula et al., 2012), ranging between 1% and 4%. NPs prepared with 1% PVA were generally preferred in the literature because the high concentration of PVA caused the bridging effect and resulted in increased NP size (Mainardes and Evangelista, 2005; Yang and Owusu-Ababio, 2000; Yerlikaya et al., 2013). TPGS is a more active surfactant than PVA (Mu and Feng, 2003a), and the concentration at which the highest encapsulation efficiency was obtained with TPGS was found to be 0.2% (Mu and Feng, 2003a; Shi et al., 2013). Therefore, we chose the concentration of TPGS as 0.2% . Additionally, the quantity of polymer and API added to the NP formation medium was adjusted in preliminary studies and the optimum NP formation was achieved with addition of maximum 3 mg of API and 5 mg of polymer.

BBB is known to be partially leaky in glioma. The increased BBB permeability may allow passage of drug-loaded NPs through the endothelium due to the enhanced permeability and retention effect (EPR). PEG-coated NPs have previously been reported to accumulate in the brain more than uncoated particles (Brigger et al., 2002; Calvo et al., 2001). Nance et al. showed that PEG-coated NPs had better penetration and distribution capacity to the brain after systemic injection and displayed improved efficiency. This effect was achieved only by the intensive coating of NPs with PEG (Nance et al., 2014; Nance et al., 2012). Encouraged by these reports, we carried out our experiments with PEGylated NPs. Additionally, PEGylation reduces PVA interaction with the NP surface, hence, facilitates the removal of PVA from NPs (Essa et al., 2010). Thus, it was possible to remove the PVA from the NPs without multiple washing.

In order to facilitate the transport of payloads of NPs, the surface of PLGA NPs are coated with surfactants or polymers (Guo and Gemeinhart, 2008). Cationic surface modification can be achieved by electrostatic interactions through the negative surface charge of PLGA NPs. The cell surface is negatively charged; therefore, the cationic particles are advantageous in terms of facilitating the interaction with the cell membrane and improving subsequent bioactivity (Guo and Gemeinhart, 2008; Mao et al., 2001). CS, a positively charged polymer, has been shown to increase permeability in addition to its mucoadhesive and controlled release properties (Artursson et al., 1994; Illum et al., 1994). Besides, positive and relatively high zeta potential of CS nanospheres are reported to cause cytotoxic effects on many tumor cell lines (Chan et al., 2007; Han et al., 2008; Ta et al., 2008; Yang et al., 2009). These features altogether make CS a preferred polymer for surface coating. Indeed, in BBB models, CS NPs were found to increase the penetration, which was associated with particle size and molecular weight; the permeability was higher with smaller particle size and lower CS molecular weight as expected (Hombach and Bernkop-Schnurch, 2009).

The reduction of particle size with PEGylation in our study can be explained by the hydrophilic nature of PEG molecules, which enabled the interaction with the aqueous phase during NP formation (Cruz et al., 2010; Nakano et al., 2007). However, when the surface was later coated with CS, the particle size of the PEGylated NPs significantly increased (approximately 70 nm). Chen et al. (Chen et al., 2009) reported that mitoxantron-loaded PLGA NPs modified with CS by both adsorption and covalent binding methods resulted in an increase in particle size of the NPs obtained depending on the CS concentration in the medium. The particle size increased due to adsorption of CS molecules, forming a layer on the surface. Similar to our findings, the increase of the particle size was close to 70 nm and this alteration was thought to be due to the interaction of surface PEG molecules and CS with hydrogen bonding (He et al., 2009).

We separately evaluated different molecular-weighted PLGA (RG 502 H, RG 503 H, RG 504 H) NPs for their surface charge. The absolute zeta potential values of the NPs prepared by TPGS were found to be significantly higher. Although TPGS is a neutral compound, NPs

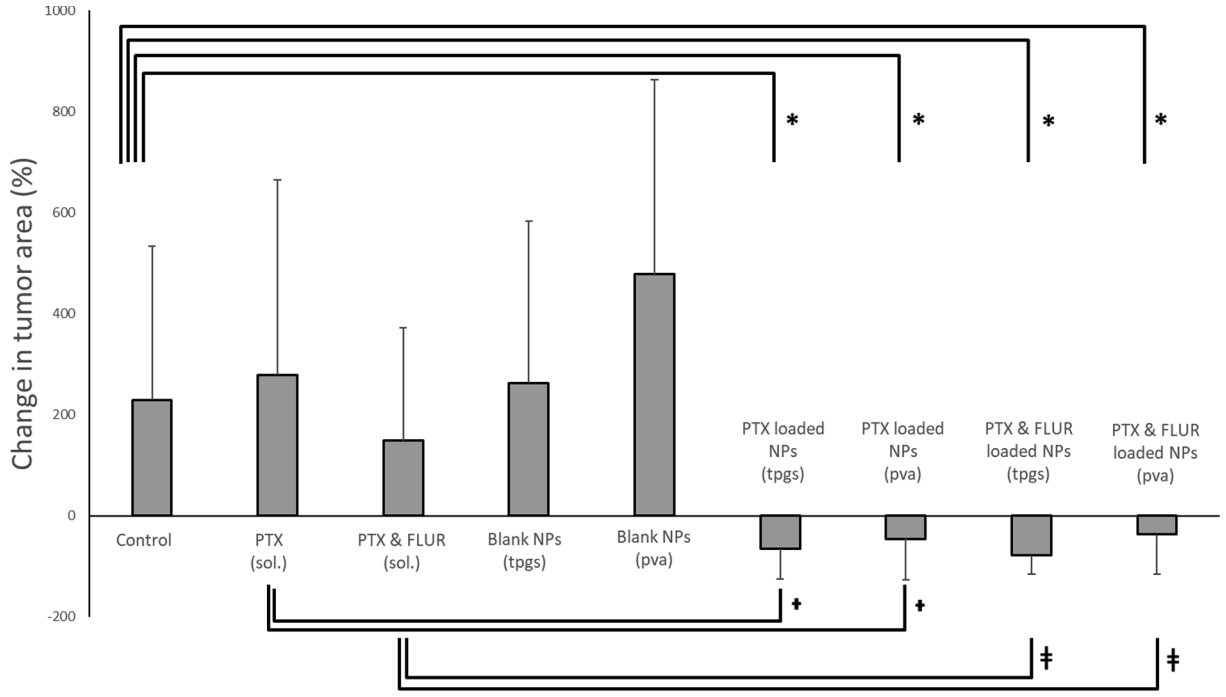

Fig. 9. The percentage change in the tumor size before and 5 days after single dose administration of NPs or their controls. The tumor growth in the rats administered with drug-loaded NPs were significantly decreased when compared with the untreated control group and rats administered API solutions (error bars = mean ± SE). Note that tumor size increased within 5 days in all control groups (five bars on the left side), whereas its growth was consistently decreased in all four treatment groups (four bars on the right side) * $p < 0.05$ compared to the untreated control group, † $p < 0.05$ paclitaxel-loaded NPs compared to the paclitaxel solution group (p values were 0.026 and 0.018 for TPGS and PVA emulsified NPs, respectively) and , ǂ $p < 0.05$ paclitaxel and R-flurbiprofen-loaded NPs compared to the paclitaxel and R-flurbiprofen solution group (p values were 0.007 and 0.014 for TPGS and PVA emulsified NPs, respectively).

prepared by TPGS may possess lower surface charge than the others because TPGS protects some of the negative charge on the surface of the NPs (Zhu et al., 2014). In the PLGA-PEG NPs coated with CS, the zeta potential values were converted from negative to positive. This finding also confirms an efficient CS coating (Chen et al., 2009). Guo et al, clarified the mechanisms of CS coating on the PLGA NPs by showing that the conversion of zeta potential to positive values indicated that the NPs were successfully coated with CS (Guo and Gemeinhart, 2008). Loading of the APIs did not cause a significant change in the surface charge of the NPs because the active substances did not provide any additional surface load owing to the absence of an ionizable structure or net charge.

PLGA NPs prepared without surface modification (RG 502 H, RG 503 H, RG 504 H) were spherical. When the surface of the NPs was

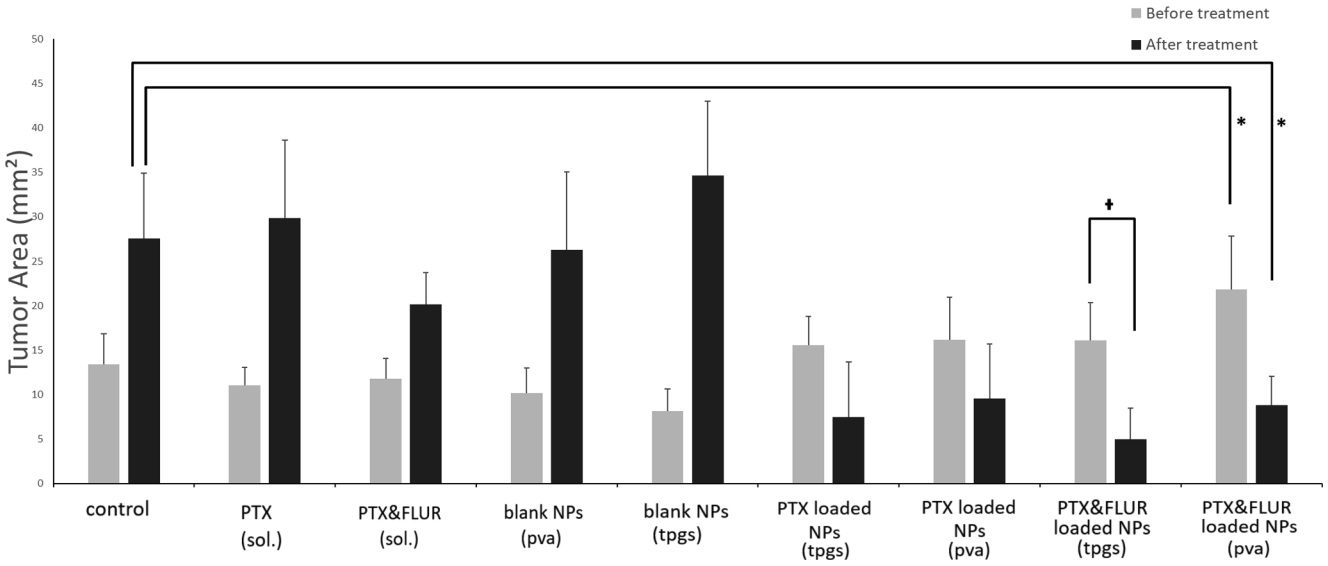

Fig. 10. The comparison of plain size of tumors on a coronal brain section before and 5 days after single dose NP administration. Both paclitaxel-loaded NPs and NP combinations reduced the tumor area. However, only the reduction in the area in combination groups (paclitaxel and R-flurbiprofen loaded NPs) reached statistical significance compared with the untreated control group. When the areas of pre-treatment and post-treatment groups were compared, only the combination group administered with the NPs emulsified with TPGS showed statistically significant change. (error bars = mean ± SE) * The groups were compared with each other in pairs, $p < 0.05$.

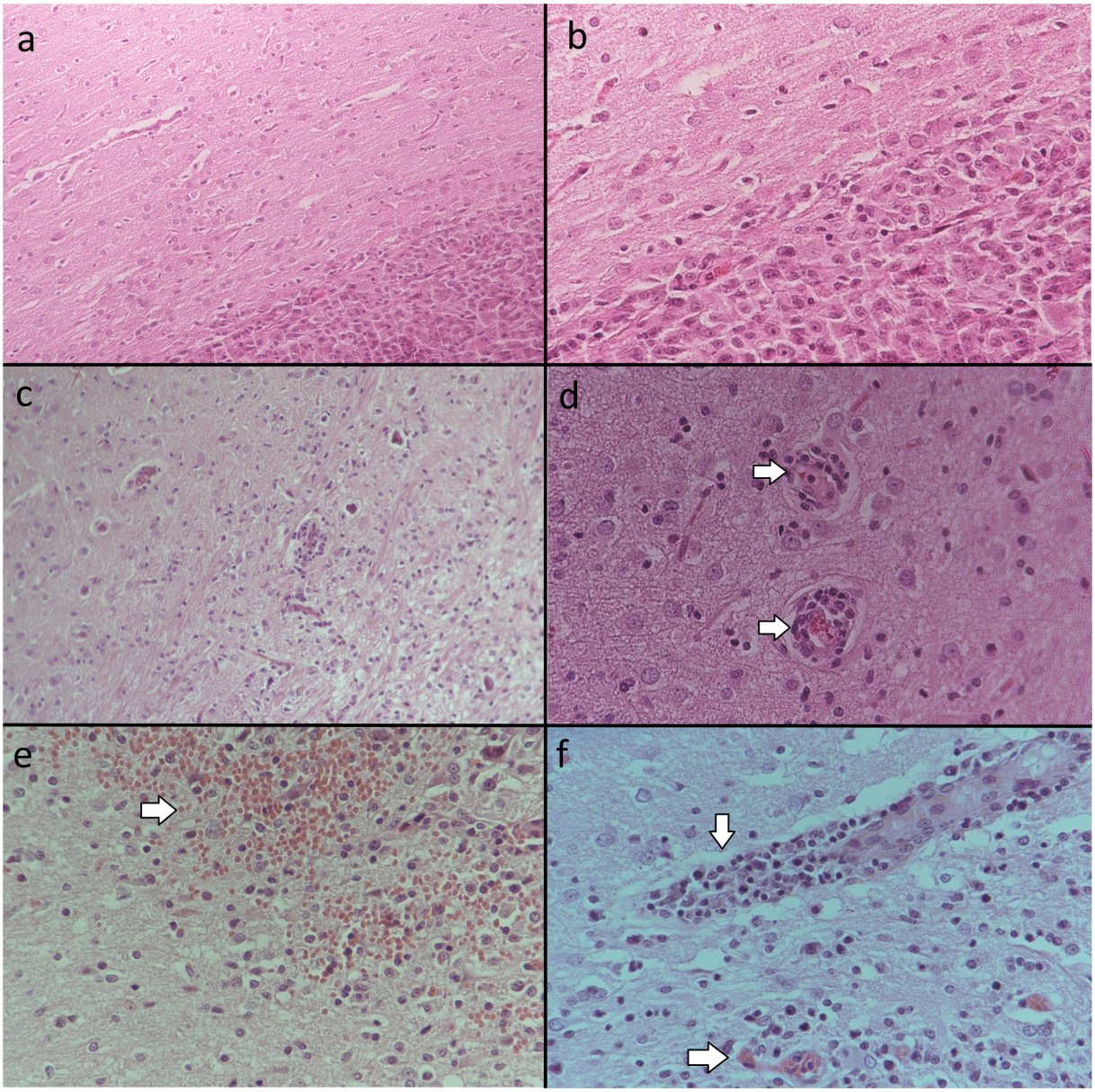

Fig. 11. Hematoxylin-Eosin stained brain sections of the post-treatment groups. The brain slices of animals treated with both paclitaxel and R-flurbiprofen NPs are shown in A and B. The inflammatory response in the *peri*-tumoral area was reduced when compared with the animals treated with the paclitaxel NPs only (C and D) or the animals administered with paclitaxel and R-flurbiprofen solution (E and F). Inflammatory cells extravasating from vascular compartment to the brain tissue and some swollen cells are visible (D). In the paclitaxel and R-flurbiprofen solution combination group, a partial hemorrhage (extravasated red blood cells) (E) and inflammatory cells around a vessel are displayed (F). (For interpretation of the references to colour in this figure legend, the reader is referred to the web version of this article.)

modified with PEG, the smooth and spherical structure of the surface slightly changed, resulting in irregularities on the surface. This finding is in line with those of Pisani et al., in which the microspheres were prepared by emulsification method using PLGA and PLGA-PEG and, the images of microspheres taken with light microscope, SEM and confocal microscope showed that the surface turned from smooth to rough when the PEGylation ratio increased (Pisani et al., 2009). Also, SEM images showed that the particles preserved their spherical shape and were physically intact, confirming that the lyophilisation did not effect the physical integrity of the NPs because the images were taken with lyophilized particles. Also, in vivo studies proved that the lyophilized particles were functionally active. Therefore, we did not further investigate the effect of lyophilization on NPs.

The encapsulation efficiency of the NPs prepared by TPGS was slightly higher than NPs prepared with PVA. In terms of encapsulation efficiency, no significant difference was observed between CS-coated formulations; only the mean of the encapsulation efficiency of the CS-coated formulations was slightly higher for paclitaxel-loaded NPs. The slower NP formation due to higher aqueous phase viscosity of CS may have resulted in a slight size increase. The encapsulation efficiency of paclitaxel was higher than R-flurbiprofen. The solubility of paclitaxel in water has been reported to be very little (estimated to be 0.00556 mg/mL) (Wishart et al., 2006). Likewise, for flurbiprofen too, the solubility in water was low and estimated to be 0.0249 mg/mL (Wishart et al., 2006). Although both molecules have low solubility, the solubility of flurbiprofen in water is about 5 times that of paclitaxel, which may have caused the molecule to move away from the hydrophobic polymer core and reduce the encapsulation efficiency. Regarding the encapsulation efficiency calculation, we separated the loaded drug from free drug by ultracentrifugation. Encouraged by similar methods used

to calculate the encapsulation efficiency in literature (Mu and Feng, 2003a; Wang et al., 2011; Xu et al., 2012; Zhang and Feng, 2006), we calculated the loaded amount directly from the lyophilized NPs. Since we did not perform further NP purification (Barichello et al., 1999), filtration (Danhier et al., 2009) or ultra-high speed centrifugation (Dalwadi and Sunderland, 2008), we might have slightly underestimated the amount loaded to NPs with particle size below 100 nm, which may not be precipitated, or overestimated it because of of APIs that may have been precipitated or adsorbed and, hence, contaminated the NP sediment due to the low aqueous solubility. Of note, we showed that chitosan coating increased the particle size of the NPs that were administered to rats during in-vivo studies. Accordingly, the NP fraction with particle size below 100 nm that could pose a risk of incomplete separation was very small. Importantly, these minor drawbacks did not lead to suboptimal dosing, as we observed a clear antitumorigenic effect with our drug-loaded NPs.

The cytotoxicity and uptake of paclitaxel or R-flurbiprofen-loaded, PLGA-PEG and CS-coated PLGA-PEG NPs were evaluated in RG2 cell culture. PLGA-PEG and CS-coated PLGA-PEG NPs containing paclitaxel showed similar cytotoxic activity compared to the control group. Similarly, Grover et al. (Grover et al., 2014) reported that docetaxel-loaded PLGA-PEG NPs were cytotoxic on RG2 cells. Janardhanan et al. tested the combination of paclitaxel and N- (4-hydroxyphenyl) retinamide on RG2 and C6 cells (Janardhanan et al., 2009). Paclitaxel at a concentration of 100 nM added to the medium resulted in death of approximately 50% of the cells. In our study, PLGA-PEG NPs with and without CS coating were added to the RG2 cell media in an amount of 5 μg (approximately 30 μM). This led to a reduction of about 40% in RG2 cell viability. Similarly, when R-flurbiprofen-loaded NPs were applied to cells at the same concentration, there was a decrease of 20–25% in RG2 cell viability. In the cellular uptake studies, we preferred PI as a marker of NP uptake because it is a membrane impermeable dye whose fluorescence is dramatically enhanced after interaction with DNA/RNA. Therefore, non-specific leakage from the NPs not taken up cannot modify the results because the extracellular PI will not emit fluorescence (Müller et al., 1991; Neumeyer et al., 2011). Also, DRAQ-7 viability dye was used to test the cellular toxicity. Upon incubation with PI-loaded NPs, the cells were harvested and DRAQ-7 dye, which emits a red fluorescence distinguishable from that of PI, was added. Then the viable cells (DRAQ-7-negative cells) were gated and analyzed for NP uptake identified by PI-positivity. Therefore we do not expect that PI staining in “control + PI” condition would be due to the cell death or loss of membrane integrity at 6 h as we monitored by DRAQ-7. On the other hand, long-term (6 h) incubation with “free PI” may have led to non-specific internalization of this dye through the intact cell membrane (Neumeyer et al., 2011). Nevertheless, unlike PI-loaded TPGS NPs, since the PI-loaded PVA NPs did not lead to an increase in the fluorescence, we may presume that the increase in control + PI condition at 6 h reflects non-specific entry of “free PI” into the cells.

When the RG2 viability values were examined, the difference between the control groups and the NPs loaded with PI (but not APIs) after 3 and 6 h was not significant. The highest level of cellular uptake was observed with NPs prepared by TPGS after 3 and 6 h incubation. In a study by Feng et al., paclitaxel was loaded to PLGA NPs and PVA or TPGS was used as a surfactant. Similarly, uptake of NPs prepared by TPGS was found to be higher in cell culture (Feng et al., 2007).

To test the functionality of two types of NPs, we used a rat model of RG2, an aggressive type of glioma, which was also used in previous studies to assess anti-tumoral activity (Sekerdag et al., 2017; Yemisci et al., 2006). Combination groups showed significant reduction in glioma growth, which indicated that the API-loaded NPs sufficiently reached to the tumor after systemic administration. Reduction in the peritumoral inflammation further supports this conclusion. In 5 control groups, tumor size significantly increased within 5 days, whereas in all treatment groups, tumor progress was halted and showed some regression. Although both NP formulations appeared to reach their target as suggested by reduced tumor sizes, the overall effect on tumor size was statistically significant only with their combined administration. This suggests that, with the dosage used, paclitaxel concentration achieved was effective but partly sufficient. However, this partial effect allowed us to see the additive effect caused by R-flurbiprofen. Such that, the combination therapy enabled not only a statistically significant decrease in tumor size but also a reduction in peri-tumoral inflammation.

The concomitant use of paclitaxel with TPGS may have been advantageous because of the P-glycoprotein inhibitory effect of TPGS (Bogman et al., 2003). Studies have shown that paclitaxel is an effective P-glycoprotein substrate and resistance to paclitaxel has been shown to depend on it (Sarisozen et al., 2012a,b). In this context, it is thought that P-glycoprotein inhibitory activity of TPGS can lead to more effective results in glioma treatment. Another advantage of our NP formulations was the reduced application dose compared to the previously used doses. In previous studies, paclitaxel was administered at a dose of 3 mg/kg for 7 consecutive days (Guo et al., 2011) or 5 mg/kg for 3 weeks, every 3 days for 1, total of 7 injections (Hu et al., 2013). Whereas in our study, 300 μg/kg of paclitaxel and 1.5 mg/kg of R-flurbiprofen were administered as a single dose. The type of cell used in our study, RG2 is a highly aggressive type of glioma and recognized in the literature as more aggressive than the C6 derivative cells used in several studies (He et al., 2013). Nevertheless, we successfully suppressed the tumor growth with our NP formulations. We administered the nanoparticular formulations via i.p. route because i.v. and i.p. administration of polymeric NPs provide similar blood concentrations. For instance, Geldenhuys et al., injected glutathione-coated and paclitaxel-loaded PLGA-PEG NPs intraperitoneally to male rats and recorded satisfactory biodistribution in the brain tissue 1 h after the intraperitoneal injection (Geldenhuys et al., 2011). Therefore, we conclude that intraperitoneal injection does not hamper passage of NPs into circulation as also reported by several previous studies (Jung et al., 2014; Yemisci et al., 2015).

Although we have shown a promising anti-glioma effect of our formulations, one of the limitations of our study is that we did not study the biodistribution of NPs, hence, their accumulation in organs like liver and spleen, where drugs used might exhibit toxicity. Future studies must investigate this point to better characterize the translational potential of our approach. Also, long-term survival studies are needed to determine if repeated dosing is required to prevent tumor recurrence. We adjusted NP dosage for rats weighing around 300 g, therefore, scale up and manufacturing process validation are needed to produce larger batches of NPs for large animal studies and eventually clinical trials.

5. Conclusion

Anti-neoplastic paclitaxel or anti-inflammatory R-flurbiprofen can efficiently be loaded to PEGylated, chitosan-modified PLGA NPs and targeted to RG2 glioma in vivo. Combination therapy with paclitaxel and R-flurbiprofen NPs exhibited enhanced anti-tumoral activity against glioma. This combination has also reduced inflammation in the peri-tumoral area. We conclude that PLGA NPs can efficiently carry their payloads to glioma tissue and the combined use of anticancer drugs with anti-inflammatory drugs exerts additional anti-tumor activity.

CRediT authorship contribution statement

Secil Caban-Toktas: Investigation, Formal analysis, Conceptualization, Methodology, Validation, Visualization, Writing - original draft. **Adem Sahin:** Investigation. **Sevda Lule:** Investigation, Formal analysis. **Güneş Esendaglı:** Investigation, Formal analysis. **Imran Vural:** Formal analysis. **Kader Karlı Oguz:** Investigation, Formal analysis. **Figen Soylemezoglu:** Formal analysis. **Melike Mut:** Formal analysis. **Turgay**

Dalkara: Writing - original draft, Writing - review & editing. **Mansoor Khan:** Writing - review & editing. **YılmazCapan:** Project administration, Supervision, Writing - review & editing.

Declaration of Competing Interest

The authors declare that they have no known competing financial interests or personal relationships that could have appeared to influence the work reported in this paper.

Acknowledgements

Funding: This research did not receive any specific grant from funding agencies in the public, commercial, or not-for-profit sectors

References

Artursson, P., Lindmark, T., Davis, S.S., Illum, L., 1994. Effect of chitosan on the permeability of monolayers of intestinal epithelial cells (Caco-2). Pharm. Res. 11, 1358–1361.
Barichello, J.M., Morishita, M., Takayama, K., Nagai, T., 1999. Encapsulation of hydrophilic and lipophilic drugs in PLGA nanoparticles by the nanoprecipitation method. Drug Dev. Ind. Pharm. 25, 471–476.
Behin, A., Hoang-Xuan, K., Carpentier, A.F., Delattre, J.Y., 2003. Primary brain tumours in adults. Lancet 361, 323–331.
Bogman, K., Erne-Brand, F., Alsenz, J., Drewe, J., 2003. The role of surfactants in the reversal of active transport mediated by multidrug resistance proteins. J. Pharm. Sci. 92, 1250–1261.
Brigger, I., Morizet, J., Aubert, G., Chacun, H., Terrier-Lacombe, M.J., Couvreur, P., Vassal, G., 2002. Poly(ethylene glycol)-coated hexadecylcyanoacrylate nanospheres display a combined effect for brain tumor targeting. J. Pharmacol. Exp. Ther. 303, 928–936.
Calvo, P., Gouritin, B., Chacun, H., Desmaele, D., D'Angelo, J., Noel, J.P., Georgin, D., Fattal, E., Andreux, J.P., Couvreur, P., 2001. Long-circulating PEGylated polycyanoacrylate nanoparticles as new drug carrier for brain delivery. Pharm. Res. 18, 1157–1166.
Chan, P., Kurisawa, M., Chung, J.E., Yang, Y.Y., 2007. Synthesis and characterization of chitosan-g-poly(ethylene glycol)-folate as a non-viral carrier for tumor-targeted gene delivery. Biomaterials 28, 540–549.
Chen, H., Yang, W., Chen, H., Liu, L., Gao, F., Yang, X., Jiang, Q., Zhang, Q., Wang, Y., 2009. Surface modification of mitoxantrone-loaded PLGA nanospheres with chitosan. Colloids and surfaces B. Biointerfaces 73, 212–218.
Cheng, J., Teply, B.A., Sherifi, I., Sung, J., Luther, G., Gu, F.X., Levy-Nissenbaum, E., Radovic-Moreno, A.F., Langer, R., Farokhzad, O.C., 2007. Formulation of functionalized PLGA-PEG nanoparticles for in vivo targeted drug delivery. Biomaterials 28, 869–876.
Claes, A., Idema, A.J., Wesseling, P., 2007. Diffuse glioma growth: a guerilla war. Acta Neuropathol. 114, 443–458.
Cruz, L.J., Tacken, P.J., Fokkink, R., Joosten, B., Stuart, M.C., Albericio, F., Torensma, R., Figdor, C.G., 2010. Targeted PLGA nano- but not microparticles specifically deliver antigen to human dendritic cells via DC-SIGN in vitro. J. Control. Release: Offic. J. Control. Release Soc. 144, 118–126.
Dalwadi, G., Sunderland, B., 2008. Comparison and validation of drug loading parameters of PEGylated nanoparticles purified by a diafiltration centrifugal device and tangential flow filtration. Drug Dev. Ind. Pharm. 34, 1331–1342.
Danhier, F., Lecouturier, N., Vroman, B., Jerome, C., Marchand-Brynaert, J., Feron, O., Preat, V., 2009. Paclitaxel-loaded PEGylated PLGA-based nanoparticles: in vitro and in vivo evaluation. J. Control. Release: Offic. J. Control. Release Soc. 133, 11–17.
Djuzenova, C.S., Fiedler, V., Memmel, S., Katzer, A., Hartmann, S., Krohne, G., Zimmermann, H., Scholz, C.J., Polat, B., Flentje, M., Sukhorukov, V.L., 2015. Actin cytoskeleton organization, cell surface modification and invasion rate of 5 glioblastoma cell lines differing in PTEN and p53 status. Exp. Cell Res. 330, 346–357.
Essa, S., Rabanel, J.M., Hildgen, P., 2010. Effect of polyethylene glycol (PEG) chain organization on the physicochemical properties of poly(D, L-lactide) (PLA) based nanoparticles. Eur. J. Pharmaceutics Biopharmaceutics: Official J. Arbeitsgemeinschaft fur Pharmazeutische Verfahrenstechnik e.V 75, 96–106.
Feng, S., Huang, G., 2001. Effects of emulsifiers on the controlled release of paclitaxel (Taxol) from nanospheres of biodegradable polymers. J. Control. Release: Offic. J. Control. Release Soc. 71, 53–69.
Feng, S.S., Zeng, W., Teng Lim, Y., Zhao, L., Yin Win, K., Oakley, R., Hin Teoh, S., Hang Lee, R.C., Pan, S., 2007. Vitamin E TPGS-emulsified poly(lactic-co-glycolic acid) nanoparticles for cardiovascular restenosis treatment. Nanomedicine (Lond) 2, 333–344.
Fitzgerald, D.P., Palmieri, D., Hua, E., Hargrave, E., Herring, J.M., Qian, Y., Vega-Valle, E., Weil, R.J., Stark, A.M., Vortmeyer, A.O., Steeg, P.S., 2008. Reactive glia are recruited by highly proliferative brain metastases of breast cancer and promote tumor cell colonization. Clin. Exp. Metastasis 25, 799–810.
Geldenhuys, W., Mbimba, T., Bui, T., Harrison, K., Sutariya, V., 2011. Brain-targeted delivery of paclitaxel using glutathione-coated nanoparticles for brain cancers. J. Drug Target. 19, 837–845.
Grosch, S., Schilling, K., Janssen, A., Maier, T.J., Niederberger, E., Geisslinger, G., 2005. Induction of apoptosis by R-flurbiprofen in human colon carcinoma cells: involvement of p53. Biochem. Pharmacol. 69, 831–839.
Grosch, S., Tegeder, I., Schilling, K., Maier, T.J., Niederberger, E., Geisslinger, G., 2003. Activation of c-Jun-N-terminal-kinase is crucial for the induction of a cell cycle arrest in human colon carcinoma cells caused by flurbiprofen enantiomers. FASEB J.: Offic. Publ. Fed. Am. Soc. Exp. Biol. 17, 1316–1318.
Grover, A., Hirani, A., Pathak, Y., Sutariya, V., 2014. Brain-targeted delivery of docetaxel by glutathione-coated nanoparticles for brain cancer. AAPS PharmSciTech 15, 1562–1568.
Guo, C., Gemeinhart, R.A., 2008. Understanding the adsorption mechanism of chitosan onto poly(lactide-co-glycolide) particles. Eur. J. Pharmaceutics Biopharmaceutics: Offic. J. Arbeitsgemeinschaft fur Pharmazeutische Verfahrenstechnik e.V 70, 597–604.
Guo, J., Gao, X., Su, L., Xia, H., Gu, G., Pang, Z., Jiang, X., Yao, L., Chen, J., Chen, H., 2011. Aptamer-functionalized PEG-PLGA nanoparticles for enhanced anti-glioma drug delivery. Biomaterials 32, 8010–8020.
Han, H.D., Song, C.K., Park, Y.S., Noh, K.H., Kim, J.H., Hwang, T., Kim, T.W., Shin, B.C., 2008. A chitosan hydrogel-based cancer drug delivery system exhibits synergistic antitumor effects by combining with a vaccinia viral vaccine. Int. J. Pharm. 350, 27–34.
He, L., Xue, R., Yang, L., Song, R., 2009. Effects of blending chitosan with PEG on surface morphology, crystallization, and thermal properties. Chinese J. of Polymer Sci. 27, 501–510.
He, T., Smith, N., Saunders, D., Pittman, B.P., Lerner, M., Lightfoot, S., Silasi-Mansat, R., Lupu, F., Towner, R.A., 2013. Molecular MRI differentiation of VEGF receptor-2 levels in C6 and RG2 glioma models. Am. J. Nucl. Med. Mol. Imag. 3, 300–311.
Hombach, J., Bernkop-Schnurch, A., 2009. Chitosan solutions and particles: evaluation of their permeation enhancing potential on MDCK cells used as blood brain barrier model. Int. J. Pharm. 376, 104–109.
Hu, Q., Gao, X., Gu, G., Kang, T., Tu, Y., Liu, Z., Song, Q., Yao, L., Pang, Z., Jiang, X., Chen, H., Chen, J., 2013. Glioma therapy using tumor homing and penetrating peptide-functionalized PEG-PLA nanoparticles loaded with paclitaxel. Biomaterials 34, 5640–5650.
Illum, L., Farraj, N.F., Davis, S.S., 1994. Chitosan as a novel nasal delivery system for peptide drugs. Pharm. Res. 11, 1186–1189.
Janardhanan, R., Butler, J.T., Banik, N.L., Ray, S.K., 2009. N-(4-Hydroxyphenyl) retinamide potentiated paclitaxel for cell cycle arrest and apoptosis in glioblastoma C6 and RG2 cells. Brain Res. 1268, 142–153.
Jung, C., Kaul, M.G., Bruns, O.T., Ducic, T., Freund, B., Heine, M., Reimer, R., Meents, A., Salmen, S.C., Weller, H., Nielsen, P., Adam, G., Heeren, J., Ittrich, H., 2014. Intraperitoneal injection improves the uptake of nanoparticle-labeled high-density lipoprotein to atherosclerotic plaques compared with intravenous injection: a multimodal imaging study in ApoE knockout mice. Circulation. Cardiovascular Imag. 7, 303–311.
King Jr., J.G., Khalili, K., 2001. Inhibition of human brain tumor cell growth by the anti-inflammatory drug, flurbiprofen. Oncogene 20, 6864–6870.
Kirby, B.P., Pabari, R., Chen, C.N., Al Baharna, M., Walsh, J., Ramtoola, Z., 2013. Comparative evaluation of the degree of pegylation of poly(lactic-co-glycolic acid) nanoparticles in enhancing central nervous system delivery of loperamide. J. Pharm. Pharmacol. 65, 1473–1481.
Mainardes, R.M., Evangelista, R.C., 2005. PLGA nanoparticles containing praziquantel: effect of formulation variables on size distribution. Int. J. Pharm. 290, 137–144.
Mao, H.Q., Roy, K., Troung-Le, V.L., Janes, K.A., Lin, K.Y., Wang, Y., August, J.T., Leong, K.W., 2001. Chitosan-DNA nanoparticles as gene carriers: synthesis, characterization and transfection efficiency. J. Control. Release: Offic. Control. Release Soc. 70, 399–421.
Mu, L., Feng, S.S., 2002. Vitamin E TPGS used as emulsifier in the solvent evaporation/extraction technique for fabrication of polymeric nanospheres for controlled release of paclitaxel (Taxol). J. Control. Release: Offic. Control. Release Soc. 80, 129–144.
Mu, L., Feng, S.S., 2003a. A novel controlled release formulation for the anticancer drug paclitaxel (Taxol): PLGA nanoparticles containing vitamin E TPGS. J. Control. Release: Offic. Control. Release Soc. 86, 33–48.
Mu, L., Feng, S.S., 2003b. PLGA/TPGS nanoparticles for controlled release of paclitaxel: effects of the emulsifier and drug loading ratio. Pharm. Res. 20, 1864–1872.
Müller, R.H., Lherm, C., Herbort, J., Couvreur, P., 1991. Propidium-iodide-loaded polyalkylcyanoacrylate particles - labelling conditions and loading capacity. Colloid Polym. Sci. 269, 147–152.
Nakano, K., Bando, Y., Tozuka, Y., Takeuchi, H., 2007. Cellular interaction of PEGylated PLGA nanospheres with macrophage J774 cells using flow cytometry. Asian J. of Pharm. Sci. 2, 220–226.
Nance, E., Zhang, C., Shih, T.Y., Xu, Q., Schuster, B.S., Hanes, J., 2014. Brain-penetrating nanoparticles improve paclitaxel efficacy in malignant glioma following local administration. ACS Nano 8, 10655–10664.
Nance, E.A., Woodworth, G.F., Sailor, K.A., Shih, T.Y., Xu, Q., Swaminathan, G., Xiang, D., Eberhart, C., Hanes, J., 2012. A dense poly(ethylene glycol) coating improves penetration of large polymeric nanoparticles within brain tissue. Sci. Transl. Med. 4, 149ra119.
Neumeyer, A., Bukowski, M., Veith, M., Lehr, C.M., Daum, N., 2011. Propidium iodide labeling of nanoparticles as a novel tool for the quantification of cellular binding and uptake. Nanomed. Nanotechnol. Biol. Med. 7, 410–419.
Pamujula, S., Hazari, S., Bolden, G., Graves, R.A., Chinta, D.D., Dash, S., Kishore, V., Mandal, T.K., 2012. Cellular delivery of PEGylated PLGA nanoparticles. J. Pharm. Pharmacol. 64, 61–67.
Parepally, J.M., Mandula, H., Smith, Q.R., 2006. Brain uptake of nonsteroidal anti-inflammatory drugs: ibuprofen, flurbiprofen, and indomethacin. Pharm. Res. 23,

873–881.
Pisani, E., Ringard, C., Nicolas, V., Raphael, E., Rosilio, V., Moine, L., Fattal, E., Tsapis, N., 2009. Tuning microcapsules surface morphology using blends of homo- and copolymers of PGA and PLGA-PEG. Soft Matter 3054–3060.
Rao, C.V., Rivenson, A., Simi, B., Zang, E., Kelloff, G., Steele, V., Reddy, B.S., 1995. Chemoprevention of colon carcinogenesis by sulindac, a nonsteroidal anti-inflammatory agent. Cancer Res. 55, 1464–1472.
Reddy, B.S., Rao, C.V., Seibert, K., 1996. Evaluation of cyclooxygenase-2 inhibitor for potential chemopreventive properties in colon carcinogenesis. Cancer Res. 56, 4566–4569.
Sarisozen, C., Vural, I., Levchenko, T., Hincal, A.A., Torchilin, V.P., 2012a. Long-circulating PEG-PE micelles co-loaded with paclitaxel and elacridar (GG918) overcome multidrug resistance. Drug Deliv. 19, 363–370.
Sarisozen, C., Vural, I., Levchenko, T., Hincal, A.A., Torchilin, V.P., 2012b. PEG-PE-based micelles co-loaded with paclitaxel and cyclosporine A or loaded with paclitaxel and targeted by anticancer antibody overcome drug resistance in cancer cells. Drug Deliv. 19, 169–176.
Sekerdag, E., Lule, S., Bozdag Pehlivan, S., Ozturk, N., Kara, A., Kaffashi, A., Vural, I., Isikay, I., Yavuz, B., Oguz, K.K., Soylemezoglu, F., Gursoy-Ozdemir, Y., Mut, M., 2017. A potential non-invasive glioblastoma treatment: Nose-to-brain delivery of farnesylthiosalicylic acid incorporated hybrid nanoparticles. J. Control. Release: Offic. Control. Release Soc. 261, 187–198.
Shi, W., Zhang, Z.J., Yuan, Y., Xing, E.M., Qin, Y., Peng, Z.J., Zhang, Z.P., Yang, K.Y., 2013. Optimization of parameters for preparation of docetaxel-loaded PLGA nanoparticles by nanoprecipitation method. Journal of Huazhong University of Science and Technology. Medical sciences = Hua zhong ke ji da xue xue bao. Yi xue Ying De wen ban = Huazhong keji daxue xuebao. Yixue Yingdewen ban 33, 754–758.
Shieh, M.J., Hsu, C.Y., Huang, L.Y., Chen, H.Y., Huang, F.H., Lai, P.S., 2011. Reversal of doxorubicin-resistance by multifunctional nanoparticles in MCF-7/ADR cells. J. Control. Release: Offic. Control. Release Soc. 152, 418–425.
Ta, H.T., Dass, C.R., Dunstan, D.E., 2008. Injectable chitosan hydrogels for localised cancer therapy. J. Control. Release: Offic. Control. Release Soc. 126, 205–216.
Tegeder, I., Niederberger, E., Israr, E., Guhring, H., Brune, K., Euchenhofer, C., Grosch, S., Geisslinger, G., 2001. Inhibition of NF-kappaB and AP-1 activation by R- and S-flurbiprofen. FASEB J.: Offic. Publ. Fed. Am. Soc. Exp. Biol. 15, 595–597.
Todoric, J., Antonucci, L., Karin, M., 2016. Targeting inflammation in cancer prevention and therapy. Cancer Prevent. Res. 9, 895–905.
Tzeng, S.Y., Green, J.J., 2013. Therapeutic nanomedicine for brain cancer. Ther. Deliv. 4, 687–704.
Vredenburgh, J.J., Desjardins, A., Reardon, D.A., Friedman, H.S., 2009. Experience with irinotecan for the treatment of malignant glioma. Neuro Oncol. 11, 80–91.
Wang, G., Yu, B., Wu, Y., Huang, B., Yuan, Y., Liu, C.S., 2013a. Controlled preparation and antitumor efficacy of vitamin E TPGS-functionalized PLGA nanoparticles for delivery of paclitaxel. Int. J. Pharm. 446, 24–33.
Wang, H., Zhao, Y., Wu, Y., Hu, Y.L., Nan, K., Nie, G., Chen, H., 2011. Enhanced antitumor efficacy by co-delivery of doxorubicin and paclitaxel with amphiphilic methoxy PEG-PLGA copolymer nanoparticles. Biomaterials 32, 8281–8290.
Wang, Y., Li, P., Kong, L., 2013b. Chitosan-modified PLGA nanoparticles with versatile surface for improved drug delivery. AAPS PharmSciTech 14, 585–592.
Wechter, W.J., Kantoci, D., Murray Jr., E.D., Quiggle, D.D., Leipold, D.D., Gibson, K.M., McCracken, J.D., 1997. R-flurbiprofen chemoprevention and treatment of intestinal adenomas in the APC(Min)/+ mouse model: implications for prophylaxis and treatment of colon cancer. Cancer Res. 57, 4316–4324.
Wechter, W.J., Leipold, D.D., Murray Jr., E.D., Quiggle, D., McCracken, J.D., Barrios, R.S., Greenberg, N.M., 2000a. E-7869 (R-flurbiprofen) inhibits progression of prostate cancer in the TRAMP mouse. Cancer Res. 60, 2203–2208.
Wechter, W.J., Murray Jr., E.D., Kantoci, D., Quiggle, D.D., Leipold, D.D., Gibson, K.M., McCracken, J.D., 2000b. Treatment and survival study in the C57BL/6J-APC(Min)/+(Min) mouse with R-flurbiprofen. Life Sci. 66, 745–753.
Wishart, D.S., Knox, C., Guo, A.C., Shrivastava, S., Hassanali, M., Stothard, P., Chang, Z., Woolsey, J., 2006. DrugBank: a comprehensive resource for in silico drug discovery and exploration. Nucleic Acids Res. 34, D668–D672.
Xu, Q., Liu, Y., Su, S., Li, W., Chen, C., Wu, Y., 2012. Anti-tumor activity of paclitaxel through dual-targeting carrier of cyclic RGD and transferrin conjugated hyperbranched copolymer nanoparticles. Biomaterials 33, 1627–1639.
Yang, Q., Owusu-Ababio, G., 2000. Biodegradable progesterone microsphere delivery system for osteoporosis therapy. Drug Dev. Ind. Pharm. 26, 61–70.
Yang, R., Shim, W.S., Cui, F.D., Cheng, G., Han, X., Jin, Q.R., Kim, D.D., Chung, S.J., Shim, C.K., 2009. Enhanced electrostatic interaction between chitosan-modified PLGA nanoparticle and tumor. Int. J. Pharm. 371, 142–147.
Yang, T., Cui, F.D., Choi, M.K., Cho, J.W., Chung, S.J., Shim, C.K., Kim, D.D., 2007. Enhanced solubility and stability of PEGylated liposomal paclitaxel: in vitro and in vivo evaluation. Int. J. Pharm. 338, 317–326.
Yemisci, M., Bozdag, S., Cetin, M., Soylemezoglu, F., Capan, Y., Dalkara, T., Vural, I., 2006. Treatment of malignant gliomas with mitoxantrone-loaded poly (lactide-co-glycolide) microspheres. Neurosurgery 59, 1296–1302 discussion 1302–1293.
Yemisci, M., Caban, S., Gursoy-Ozdemir, Y., Lule, S., Novoa-Carballal, R., Riguera, R., Fernandez-Megia, E., Andrieux, K., Couvreur, P., Capan, Y., Dalkara, T., 2015. Systemically administered brain-targeted nanoparticles transport peptides across the blood-brain barrier and provide neuroprotection. J. Cereb. Blood Flow Metab. 35, 469–475.
Yerlikaya, F., Ozgen, A., Vural, I., Guven, O., Karaagaoglu, E., Khan, M.A., Capan, Y., 2013. Development and evaluation of paclitaxel nanoparticles using a quality-by-design approach. J. Pharm. Sci. 102, 3748–3761.
Zhang, Z., Feng, S.S., 2006. The drug encapsulation efficiency, in vitro drug release, cellular uptake and cytotoxicity of paclitaxel-loaded poly(lactide)-tocopheryl polyethylene glycol succinate nanoparticles. Biomaterials 27, 4025–4033.
Zhu, H., Chen, H., Zeng, X., Wang, Z., Zhang, X., Wu, Y., Gao, Y., Zhang, J., Liu, K., Liu, R., Cai, L., Mei, L., Feng, S.S., 2014. Co-delivery of chemotherapeutic drugs with vitamin E TPGS by porous PLGA nanoparticles for enhanced chemotherapy against multi-drug resistance. Biomaterials 35, 2391–2400.